Journal of Pharmaceutical Sciences 108 (2019) 1423-1433

Contents lists available at ScienceDirect

Journal of Pharmaceutical Sciences

journal homepage: www.jpharmsci.org

Pharmaceutical Biotechnology

Lyophilization Process Design and Development: A Single-Step Drying Approach

Swapnil K. Pansare, Sajal M. Patel*

MedImmune, LLC, Dosage Form Design and Development Gaithersburg, Maryland 20878

ARTICLE INFO

Article history:
Received 5 September 2018
Revised 6 November 2018
Accepted 14 November 2018
Available online 20 November 2018

Keywords:
lyophilization
freeze-drying
drying
protein formulation(s)
stability
viscosity
physical stability
chemical stability

ABSTRACT

High-throughput lyophilization process was designed and developed for protein formulations using a single-step drying approach at a shelf temperature (T_s) of ≥40°C. Model proteins were evaluated at different protein concentrations in amorphous-only and amorphous-crystalline formulations. Single-step drying resulted in product temperature (T_p) above the collapse temperature (T_c) and a significant reduction (of at least 40%) in process time compared to the control cycle (wherein $T_p < T_c$). For the amorphous-only formulation at a protein concentration of ≤25 mg/mL, single-step drying resulted in product shrinkage and partial collapse, whereas a 50 mg/mL concentration showed minor product shrinkage. The presence of a crystallizing bulking agent improved product appearance at ≤25 mg/mL protein concentration for single-step drying. No impact to other product quality attributes was observed for single-step drying. Vial type, fill height, and scale-up considerations (i.e., choked flow, condenser capacity, lyophilizer design and geometry) were the important factors identified for successful implementation of single-step drying. Although single-step drying showed significant reduction in the edge vial effect, the scale-up considerations need to be addressed critically. Finally, the single-step drying approach can indeed make the lyophilization process high throughput compared to traditional freeze-drying process (i.e., 2-step drying).

Introduction

Since the introduction of recombinant DNA technology, the number of therapeutic biologics has increased significantly in the last 2 decades. In addition, recent biologics are developed in more complex formats, such as fusion proteins, bispecific monoclonal antibodies, and antibody drug conjugates. For these non-monoclonal antibody (non-mAb) therapeutics and mAbs with significant stability issues, achieving liquid stability is challenging and, hence, a lyophilized drug product presentation remains a practical option for parenteral drug products. Typically, the lyophilization process involves 3 steps: (1) freezing: to convert water into ice; (2) primary drying: to remove ice via sublimation; and (3) secondary drying: where unfrozen water is removed via desorption.[1] Lyophilization unit operation can be time and energy intensive depending on the process design. To achieve the goal of bringing quality drug products to patients more quickly, improving process efficiency is now a major emphasis.[2] Unit operations such as lyophilization may provide an opportunity to significantly reduce the manufacturing time and cost by optimization of the process parameters. In addition, based on therapeutic area and target patient population, some products may require manufacturing a larger drug product lot size, which would require a large production-scale freeze dryer and multiple drug product lots per year to meet the commercial demand. Reducing the freeze-drying process time would be prudent to support such needs.

In general, liquid drug product is preferred due to dose administration convenience, cost effectiveness, and throughput. However, as mentioned earlier, achieving liquid stability for a commercial shelf life may be challenging for certain biologics and, hence, lyophilized drug product is preferred because lyophilization is an established aseptic manufacturing process within the industry. Alternatives to freeze-drying have been explored (e.g., spray drying, spray freeze drying, foam drying, vacuum drying, microglassification, and microwave drying),[3-7] which may lower the cost and increase the throughput for drug product manufacturing.

Abbreviations used: CM, capacitance manometer; dm/dt, sublimation rate; FDM, freeze-dry microscopy; HPSEC, high-performance size-exclusion chromatography; IgG1, immunoglobulin G type 1; mAb, monoclonal antibody; OCT-FDM, optical coherence tomography freeze-dry microscopy; $P_{c,min}$, minimum achievable chamber pressure without losing chamber pressure control; SVFD, single-vial freeze dryer; T_c, collapse temperature determined by freeze-dry microscopy; T_g, glass transition temperature of a solid; T_g', glass transition temperature of the maximally freeze-concentrated solution; T_s, shelf temperature; T_p, product temperature; $T_{p,max}$, maximum allowable product temperature; $T_{p,avg}$, average product temperature; $T_{p,ss}$, average steady-state product temperature.

* *Correspondence to:* Sajal M. Patel (Telephone: +1-301-398-5247).
E-mail address: PatelSaj@medimmune.com (S.M. Patel).

https://doi.org/10.1016/j.xphs.2018.11.021
0022-3549/

Unfortunately, these processes are not yet fully established for routine production of clinical and commercial lots of parenteral drug products. If the length of the lyophilization cycle can be reduced significantly (e.g., to a 1-day cycle), then the lyophilization process may also become high throughput and cost effective compared to these alternate drying techniques.

Optimization of the freeze-drying process is important to reduce drug product manufacturing time and cost.[8,9] Primary drying is often the longest step of the freeze-drying process, and, hence, optimization of this step is the focus in industry.[10,11] The key constraint in primary drying optimization is the product temperature (T_p), which typically needs to be maintained below the glass transition temperature of the maximally freeze-concentrated solution (T_g') and the collapse temperature (T_c).[9,10,12] As reported in the literature,[13,14] performing primary drying with the T_p above the T_g' or T_c may result in product collapse or melt back, which may negatively affect product quality attributes such as reconstitution time, residual water, and stability. In general, for low concentration amorphous formulations (<50 mg/mL), the T_c is within 1°C-2°C of the T_g', whereas for high concentration amorphous formulations (≥50 mg/mL), a significant difference between T_c and T_g' is observed.[8,9,12] The difference in T_c and T_g' for high-concentration protein formulations (≥50 mg/mL) allows primary drying to be performed significantly above T_g', but below T_c, without impacting product quality (including product appearance). The approach of drying above T_g' and below T_c has been used to improve process efficiency for high-concentration protein formulations.[9] In addition, recent studies have reported no significant difference in drug product stability even for a completely collapsed product compared to an elegant product.[15-17] Independent of the criticality of product appearance, can the product be dried above T_c and still maintain acceptable product appearance? To address this important question from a process development perspective, the T_c measured by freeze-dry microscopy (FDM) needs to be lower than the temperature at which collapse is observed in the primary container (vial, dual chamber syringe, and so forth) during the lyophilization process. This difference in the T_c may be due to difference in sample volume (i.e., a thin film with a few μL of sample under FDM compared to several mL in a vial) resulting in differences in nucleation temperature, crystallization of ice and solutes, and drying rate.[18,19] Recent advances in technology have enabled determination of the T_c in a vial during the lyophilization process using a single-vial freeze dryer along with optical coherence tomography (called optical coherence tomography freeze-dry microscopy). This technique has indicated that the T_c in a vial can be significantly higher (at least 3°C higher for a 5% sucrose solution) compared to FDM.[18-20] This difference is significant with regard to lyophilization process optimization because every 1°C increase in T_p during primary drying results in about a 13% reduction in the primary drying time.[10]

Developing efficient freeze-drying cycle has been a goal within industry for many years. Empirical and numerical modeling approaches for optimizing lyophilization process have been reported extensively in the literature.[21-25] Optimization of the freeze-drying process by varying the shelf temperature (T_s) and chamber pressure during the primary drying step has also been discussed in the literature.[9,10,25-28] In addition, previous single-step drying approach (i.e., primary and secondary drying performed in 1 step) evaluated a sucrose/glycine formulation matrix at a 100 mg/mL protein concentration.[29] The difference between chamber pressure and vapor pressure of ice at the sublimation front was used to design an efficient process by keeping the T_s as high as possible, while maintaining the T_p below T_g'.[29]

The objective of the present work is to demonstrate application of single-step drying via 2 industry case studies: a mAb and a fusion protein. Assessment of impact on process performance and product quality is presented across a range of formulation matrix. In addition, single-step drying was performed by combining primary and secondary drying in 1 step, and the T_p during drying was maintained above T_c, as measured by FDM, to assess the impact on product quality. A control cycle with $T_p < T_c$ using 2-step drying (i.e., primary and secondary drying) was performed for comparison (details in Table 1). The chamber pressure (P_c) for both single-step drying and the control cycle was kept constant throughout the drying step. Amorphous-only and amorphous-crystalline formulation matrices were evaluated at different protein concentrations for both single-step drying and the control cycle. Lyophilized formulation optimization has been discussed in the literature[1,10,30] and is outside the scope of this article. The focus of this article is primarily on freeze-drying process optimization.

Materials and Methods

Materials

Proteins used in this study were manufactured and purified at MedImmune (Gaithersburg, MD) using proprietary methods. Three model proteins used for this study were mAb A and mAb C, which are IgG1 mAbs; and Pro B, which is a fusion protein. Model proteins, mAb A and Pro X are susceptible to undergo significant degradation (both aggregation and fragmentation) in the solution at an elevated temperature (40°C). The mAb C was used as a model protein only for the scale-up evaluation study performed for amorphous-only formulation matrix (Table 1) and no stability study was performed. mAb A and Pro B were used to evaluate the effect of single-step drying for both the amorphous-only and amorphous-crystalline formulation matrices (Table 1).

For the amorphous-only formulation matrix, mAb A, mAb C, and Pro B were formulated in a buffered solution with disaccharide sugar (7% to 8% w/v) and surfactant as excipients. mAb A was prepared at protein concentrations of 10, 25, and 50 mg/mL, whereas mAb C and Pro B were prepared at a protein concentration of 50 mg/mL.

For the amorphous-crystalline formulation matrix, mAb A and Pro B were formulated at 2.5 and 25 mg/mL protein concentrations in a buffered solution with crystallizing excipient (2% w/v) and disaccharide sugar (1% w/v) in a ratio of 2:1. As outlined in prior studies,[31,32] bulking or crystallizing excipients are used to optimize the freeze-drying process, and a similar approach was used in this study to show application of single-step drying process for low protein concentration formulation (≤25 mg/mL).

Vials with 3, 10, and 20 mL capacity (type 1 glass tubing vials) and the corresponding size single-vent lyophilization stoppers were used (Table 1). Vials and stoppers were obtained from West Pharmaceutical Services, Inc. (Exton, PA).

Lyophilization Process

Drug product presentations listed in Table 1 were used for lyophilization of the model proteins. Before the freeze-drying run, the vials were partially stoppered with 13 mm (for 3-mL and 2R vials) or 20 mm (for 10-mL and 20-mL vials) lyophilization stoppers. Lyophilization cycles were performed using a Lyostar III or Virtis Genesis 35 EL (SP Scientific, Stone Ridge, NY) or Millrock PDQ24XS-S (Millrock Technology, Kingston, NY) freeze dryers. Freeze-drying process parameters used for single-step drying and control cycles are listed in Table 1.

Table 1
Experimental Design, Process Data, and Thermal Characterization Results

Protein[a]	T_c (°C)	T_g' (°C)	Vial Size	Fill Volume (mL)	Cycle ID[b]	Drying T_s (°C)[c]	Drying Ramp Rate (°C/min)[d]	$T_{p,avg}$ (°C)	$T_{p,ss}$ (°C)	Total Drying Time[f] (h)	Stability Performed?	Parameter Evaluated
Amorphous-only formulation												
mAb A 50 mg/mL	−21	−26	3-mL	1.1	50-A-SS	60	0.5	−3.5	−13.9	6.8	Yes	Protein concentration
					50-A-C	0	0.5	−20.1	−20.0	17.0		
mAb A 25 mg/mL	−28	−28	3-mL	1.1	25-A-SS	60	0.5	−1.8	−20.2	7.2	Yes	Protein concentration
					25-A-C	−20	0.5	−27.5	−27.0	27.8		
mAb A 10 mg/mL	−33	−34	3-mL	1.1	10-A-SS	60	0.5	5.5	NA	6.4	Yes	Protein concentration
					10-A-C	−30	0.5	−33.4	−27.7	59.6		
mAb A 50 mg/mL	−21	−26	3-mL	1.1	50-A-R	60	0.1	−15.9	−15.8	24.2	No	Ramp rate
					50-A-SS	60	0.5	−3.5	−13.9	6.8		
Pro B 50 mg/mL	−20	−25	10-mL	3.3	50-B-10	60	0.5	−1.2	−13.5	8.2	No	Vial type
			20-mL	5.5	50-B-20	60	0.5	−3.5	−12.3	7.1		
Pro B 50 mg/mL	−20	−25	10-mL	7.7	50-B-7.7	60	0.5	1.0	−10.1[h]	17.2	No	Fill height
			10-mL	3.3	50-B-3.3	60	0.5	−1.2	−13.5	7.9		
Pro B 50 mg/mL	−20	−25	20-mL	5.5	50-B-SS	40	0.5	−4.5	−14.9	21.0	Yes	Pilot scale
			20-mL	5.5	50-B-C	0	0.5	−19.0	−19.8	37.0		
mAb C 50 mg/mL	−19	−26	2R	1.2	50-MC-L	40	0.3	−9.4	−16.5	10.0	No	Scale-up[e]
			3-mL	1.2	50-MC-P	40	0.3	−7.2	−16.0	9.0		
Amorphous-Crystalline Formulation												
mAb A 2.5 mg/mL[g]	−18	NP	3-mL	1.1	2.5-AC-SS	60	0.5	−6.5	−18.0	5.0	Yes	Protein concentration
					2.5-AC-C	0	0.5	−21.9	−20.4	9.5		
mAb A 25 mg/mL	−16	NP	3-mL	1.1	25-AC-SS	60	0.5	−5.9	−11.8	5.4	Yes	Protein concentration.
					25-AC-C	0	0.5	−22.0	−22.0	11.4		
Pro B 2.5 mg/mL[g]	−17	NP	3-mL	1.1	2.5-BC-SS	60	0.5	−6.3	−18.0	5.0	Yes	Protein concentration
					2.5-BC-C	0	0.5	−21.3	−20.4	9.5		
Pro B 25 mg/mL	−15	NP	3-mL	1.1	25-BC-SS	60	0.5	−7.4	−11.0	5.5	Yes	Protein concentration
					25-BC-C	0	0.5	−21.5	−22.5	11.6		

T_c, collapse temperature; T_g', glass transition temperature; T_s, shelf temperature; $T_{p,avg}$, average product temperature which is determined from start of drying step (including ramp phase) to when T_p reached within 3°C of T_s; $T_{p,ss}$, average steady-state product temperature; NP, not performed; NA, not applicable (steady state was not observed).

[a] mAb A and mAb C are IgG1 monoclonal antibodies. Pro B is a fusion protein with a molecular weight of ~90 kDa.

[b] Cycle ID key: C, control; L, laboratory scale; P, pilot scale; R, ramp rate; SS, single-step drying.; A, mAb A; B, Pro B; MC, mAb C; AC, and BC, mAb A and Pro B in amorphous-crystalline formulation, respectively.

[c] T_s was constant for both the primary and secondary drying phases of the single-step drying. For the control cycle, the T_s for the primary drying step was as listed in the table; for the secondary drying, the T_s was 40°C for 6 h.

[d] For the control cycle, the drying ramp rate is for the primary drying step.

[e] From laboratory scale to pilot scale.

[f] Total drying time includes drying ramp and hold and end of drying was determined when T_p reached within 3°C of T_s.

[g] Single-step drying and control cycle were performed by combining the vials for mAb A and Pro B in a single freeze-drying run.

[h] $T_{p,ss}$ was determined for a brief steady state before the dip in the product temperature.

Differential Scanning Calorimetry

A differential scanning calorimeter (Q2000 series) from TA instruments (New Castle, DE) was used for T_g' and T_g measurements. A sample volume of 20 μL was used in an aluminum pan sealed hermetically. An empty pan without any sample along with the lid was used as the reference. Liquid samples were frozen to −60°C at a ramp rate of 5°C/min with an equilibrium time of 5 min at −60°C, then heated to 25°C at a ramp rate of 5°C/min. The T_g determination for the lyophilized product was performed using ~5 mg of sample sealed into an aluminum pan and analyzed in a conventional differential scanning calorimetry (DSC) mode. Pans were heated at a 25°C/min ramp rate to 150°C. Ramp rate of 25°C and 5°C/min were used for T_g and T_g' determination, respectively, based on DSC method optimization to get the sharp glass transition endotherm.[33,34] Universal Analysis software was used to determine the T_g' and T_g. Midpoint T_g' and T_g values are reported as the glass transition temperature.

Freeze-Dry Microscopy

All samples were tested using an Olympus BX50 microscope with a Linkam FDCS 196 stage. A freeze-dry microscope with a QImaging camera attachment was used for recording images. A sample volume of 5-10 μL was used for analysis. Sample was placed between 2 cover slips on the FDM stage. During the first step, sample was cooled and frozen to −40°C, followed by annealing at −16°C, followed by refreezing to −40°C. A ramp rate of 10°C/min was used throughout the freezing steps. After freezing, a vacuum of 150 mTorr was applied using a vacuum pump, and then the FDM stage temperature was increased at a ramp rate of 1°C/min. When the temperature reached the *Tg*', the ramp rate was decreased to 0.5°C/min. The onset of collapse was observed as bright visible holes or lack of structure in the dried matrix and was recorded as the T_c.

High-Performance Size-Exclusion Chromatography

High-performance size-exclusion chromatography (HPSEC) analysis was performed using an Agilent high-performance liquid chromatography system by measuring UV absorbance at 280 nm. For HPSEC analysis, a TSKgel G3000SW$_{XL}$ column (7.8 mm × 300 mm) was used along with TSKgel SW$_{XL}$ guard column (6.0 mm × 40 mm) from Tosoh Bioscience (King of Prussia, PA). A mobile phase composed of 0.1 M sodium phosphate, 0.1 M sodium sulfate, 0.05% (w/v) sodium azide, pH 6.8 was used (for Pro B, the mobile phase was 90% of this solution along with 10% isopropanol). Formulations at 25 and 50 mg/mL were diluted to 10 mg/mL with phosphate buffered saline (Gibco Life Technologies Corp., Grand Island, NY) before the analysis, and 25 μL of sample was injected. Formulations at 10 mg/mL were injected neat with an injection volume of 25 μL. Formulations at 2.5 mg/mL were injected with an injection volume of 100 μL to maintain constant protein load. The flow rate was 1 mL/min, and samples were held at 5°C in the auto sampler tray before injection. The relative percentage of each species for all samples (aggregates, monomer, and fragments) was calculated relative to the total area of all peaks.

Microflow Imaging

Subvisible particle (SVP) analysis was performed by microflow imaging (MFI) technique using an MFI 5200 instrument from Protein Simple (Santa Clara, CA). Samples were analyzed without dilution. Before each measurement, the background illumination was optimized using the sample itself. Approximately 0.25 mL sample was allowed to flow through before counting SVPs. Counts for particle sizes ≥2 μm, ≥ 10 μm, and ≥25 μm were recorded for particles with an aspect ratio less than 0.85. SVP analysis was performed for stability samples (as per Table 1) for Time T = 0 and end of stability study (T = 3.5 and 2 years for amorphous and amorphous-crystalline formulation matrix samples, respectively). Increase in SVP counts/mL is shown by subtracting T0 counts from end of stability samples. Time T = 0 lyophilized samples were frozen at −20°C and thawed at the end of stability study for MFI analysis.

Moisture Determination

A Karl Fischer (KF) coulometer (models: Mettler Toledo DL39 and C30, Columbus, OH) was used to determine the residual moisture. For model C30, KF titrator equipped with a Stromboli oven sample changer was used for residual moisture measurement.[35] For model DL39, lyophilized product was reconstituted with anhydrous methanol, then mixed and injected into the KF coulometer. Determination of the residual moisture content was based on the amount of water titrated relative to the mass of the lyophilized sample.

Potency Determination

In vitro potency of mAb A and Pro B was measured using an in-house cell-based assay specific for each protein. For both proteins, the potency was measured by the ability of the protein to inhibit binding of the respective molecule target to cells expressing a luciferase reporter gene. Luciferase expression was quantified using a chemiluminescent substrate and a Perkin Elmer Envision plate reader. The amount of luminescence signal measured after reaction with the substrate was proportional to the quantity of live cells following incubation with the sample. Potency results for mAb A and Pro B were expressed as percent potency relative to a reference standard (nonlyophilized).

Capillary Isoelectric Focusing

Capillary isoelectric focusing (cIEF) analysis was performed for Pro B to detect changes in charged variants. Pro B samples were diluted to 2 mg/mL and 8 mg/mL with ultrapure water. An 8 μL volume of Pro B samples was mixed with 200 μL of a buffer master mix containing urea, ultrapure water, 1% methyl cellulose, pharmalyte, and pI markers. All samples were analyzed using an iCE280 or iCE3 (ProteinSimple) by focusing for 1 min and 10 min at 1500V and 3000V, respectively.

Stability Studies

Stability of lyophilized drug product was evaluated at intended storage temperature of 2°C-8°C and at stressed condition of 40°C for mAb A and Pro B for both control and single-step drying cycles (Table 1). No studies were performed at 25°C, as 40°C temperature was deemed sufficient to understand impact of single-step drying process on product quality. A visual inspection of the lyophilized product was performed at each time point. Lyophilized vials were reconstituted using sterile water for injection, and reconstitution time was measured at various time points. Post reconstitution samples were analyzed for purity by HPSEC for mAb A and Pro B. In addition, selected time point samples were analyzed for potency by luciferase reporter gene assay and chemical stability by cIEF.

Physical and Thermal Characterization of the Product During Single-Step Drying

Using a sample thief, vials were stoppered on the shelf at various time points during the single-step drying (mAb A, cycle ID: 50-A-SS, Table 1). Stoppered vials were in a tight hexagonal array surrounded by vials undergoing drying. For the vials with melt back (referred as G1 and G2 vials in the Results and Discussion section), the water content was determined by gravimetric method, whereas for the vials with lyophilized product (referred as G3, G4, G5 and G6 vials in Results and Discussion section), the residual water was determined by KF. In addition, T_c was determined for vials containing the solution, whereas T_g was determined for vials with product. A maximum allowable temperature ($T_{p,max}$) curve was created using T_c and T_g for single-step drying. Osmolality, protein concentration, T_g', and viscosity measurements were performed for prelyo sample (referred as G0) and vials with melt back (i.e., G1 and G2 vials that contained solution).

Scale-Up Considerations

Pro B at 50 mg/mL in amorphous-only formulation was used to evaluate the scale-up considerations for single-step drying as a case study. The minimum achievable chamber pressure ($P_{c,min}$) without losing chamber pressure control in the absence of air leak[36,37] and the sublimation rate (dm/dt) were determined to evaluate choked flow challenge for the single-step drying process. Determination of $P_{c,min}$ and dm/dt was performed for different T_s on a laboratory-scale lyophilizer (Virtis) as per the method reported in the literature (using bottomless trays with distilled water).[38]

Results and Discussion

Thermal Analysis (T_c and T_g' Measurement)

As shown in Table 1, for mAb A in the amorphous-only formulation, an increase in protein concentration resulted in an increase in both T_g' and T_c. As expected,[9,12] for mAb A and Pro B, at least a 5°C difference in T_g' and T_c was observed at the 50 mg/mL protein concentration. For the amorphous-crystalline formulation, mAb A and Pro B showed an increase in the T_c with an increase in protein concentration from 2.5 to 25 mg/mL (Table 1).

Lyophilization Process Data

mAb A, Pro B, and mAb C were lyophilized using single-step drying and control cycles. Representative lyophilization process data are shown in Figures 1a and 1b for Pro B at 25 mg/mL in the amorphous-crystalline formulation.

Comparison of Product Temperature Profile

The T_p profile for edge and center vial measured using thermocouples for single-step drying and the control cycle is shown in Figure 1a. The control cycle (cycle ID: 25-BC-C) had an average steady-state product temperature ($T_{p,ss}$) of −22.5°C, which is below the collapse temperature (T_c = −15°C, Table 1), whereas, for single-step drying (cycle ID: 25-BC-SS), the $T_{p,ss}$ was −11°C, which is above the T_c. The T_p for the single-step drying dipped after reaching a brief steady-state period (Fig. 1a), which may be indicative of micro-collapse.[9,18] The control cycle showed significant difference in the T_p of the center and edge vials, indicating heterogeneity in the drying rate (Fig. 1a). Conversely, for the single-step drying, the center and edge vials completed drying at about the same time, indicating homogeneity in the drying rate.

Comparison of Pressure Profile

The capacitance manometer-Pirani differential was used to determine the end of drying[11] for single-step drying and the control cycle (Fig. 1b). The Pirani profile toward end of the single-step drying showed a steep drop in pressure (slope: ~124 mTorr/h) compared to the control cycle (slope: ~36 mTorr/h). The slope of the Pirani pressure drop is an indicator of batch homogeneity, where a steeper slope (i.e., a higher slope value) indicates homogenous drying of the batch.[35] Based on the Pirani pressure profile, single-step drying showed comparatively higher batch homogeneity in drying compared to the control cycle. In addition, single-step drying showed a significant decrease in the total drying time (>50%) compared to the control cycle.

For all the conditions evaluated (Table 1), comparison of the single-step drying and control cycles showed a similar trend for T_p and the Pirani profile (Figs. 1a and 1b). The moisture content was similar among all lyo cycles at less than 1% (range: 0.4%-0.8%). Overall, single-step drying resulted in a significant decrease (at

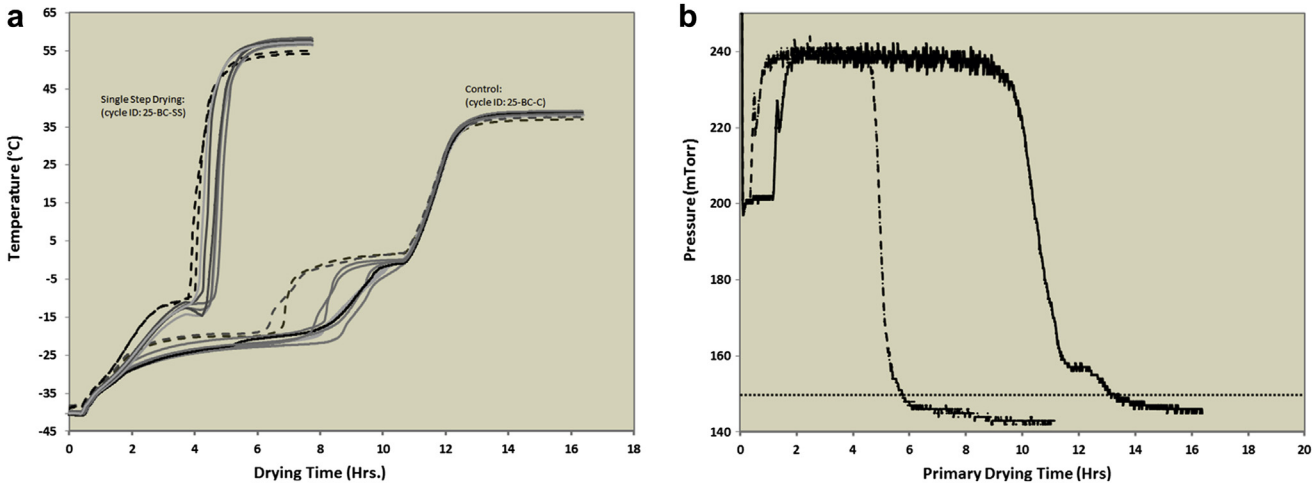

Figure 1. For Pro B at 25 mg/mL in amorphous-crystalline matrix, panel a is showing comparison of (T_p) data from thermocouples inserted into different locations of the vial array for single-step drying and control cycle. Center thermocouple vials are represented by solid line, whereas dotted line represents edge thermocouple vials. Panel b is showing comparison of the Pirani pressure profile for single-step drying (dashed line) and control cycle (solid line) with capacitance manometer (CM) (dotted line).

least 40%) in drying time compared to the control cycle for all the parameters evaluated for mAb A and Pro B (Table 1).

Visual Lyophilized Product Appearance: Amorphous-Only Formulation Matrix

Lyophilized product from the control cycle for mAb A at 10, 25, and 50 mg/mL (cycle IDs: 10-A-C, 25-A-C, and 50-A-C, respectively) resulted in an elegant appearance, whereas the single-step drying cycles showed the product shrinkage with the 50 mg/mL (cycle ID: 50-A-SS) and 25 mg/mL protein concentration (cycle ID: 25-A-SS). In addition, single-step drying of mAb A at 10 mg/mL (cycle ID: 10-A-SS) showed partial collapse and shrinkage (Fig. 2). For mAb C at 50 mg/mL (cycle ID: 50-MC-L, 50-MC-P), single-step drying resulted in shrinkage similar to mAb A at 50 mg/mL. For Pro B at 50 mg/mL, single-step drying cycles (cycle IDs: 50-B-3.3, 50-B-10 and 50-B-20) showed presence of cracks in the dried product. Although single-step drying cycle for 10 and 25 mg/mL mAb A formulation showed partial collapse and shrinkage (likely resulting in differences in specific surface area), no impact on physical and chemical stabilities was observed (discussed in the following sections) and hence additional characterization was deemed unnecessary.

Product shrinkage and cracking, as observed for amorphous-only formulation, is a potential way by which the stress built up during drying is relieved.[2,39] Lyophilized product with shrinkage and partial collapse may be acceptable as long as there is no impact on any critical product quality attributes.[2] However, to define what product appearance is acceptable, is outside the scope of this work, and is summarized in the literature.[2]

Visual Lyophilized Product Appearance: Amorphous-Crystalline Formulation Matrix

Lyophilized product for mAb A and Pro B at 2.5 and 25 mg/mL from the single-step drying and control cycles showed elegant appearance with no product defects (similar to Figs. 2, 50 mg/mL control cycle).

Post Reconstitution Appearance

For all the conditions tested (Table 1), single-step drying and control cycle, lyophilized product on reconstitution showed no visible particles and no change in color and clarity on stability.

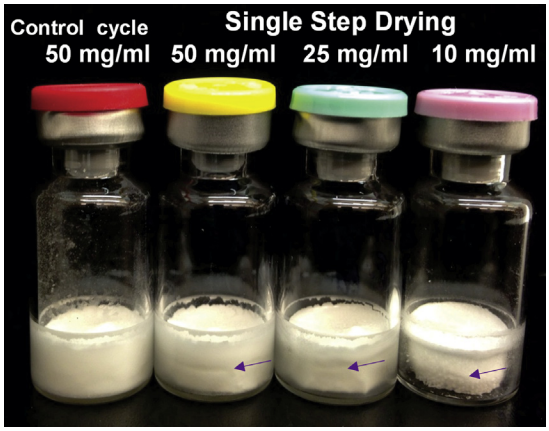

Figure 2. Lyophilized product appearance for effect of protein concentration of mAb A formulations at 50, 25, and 10 mg/mL in amorphous-only formulation matrix. First vial from left is the representative product appearance for control cycle at 50 mg/mL and rest of the vials are from single-step drying at 50, 25, and 10 mg/mL. Areas of product shrinkage and partial collapse are noted by the arrows.

Stability of Lyophilized Samples

Lyophilized samples from single-step drying and control cycles were placed on stability at 2 temperatures, 5°C and 40°C, and were evaluated for physical and chemical stabilities at various time points. Stability was evaluated for the model proteins mAb A and Pro B in amorphous-only and amorphous-crystalline formulations at different protein concentrations (10, 25, and 50 mg/mL for the amorphous-only formulation for mAb A and 2.5 and 25 mg/mL for the amorphous-crystalline formulation for mAb A and Pro B).

For stability studies at 5°C and 40°C, no physical changes were observed in lyophilized product appearance at the various time points, and the appearance was comparable to post lyophilization. In addition, no significant difference in aggregation rates was observed based on 12 months of data at 5°C and 1-2 months of data at 40°C (Table 2). mAb A and Pro B lyophilized product at 50 mg/mL showed reconstitution time in the range of 3 to 9 min for all storage time and temperature conditions. Reconstitution time for mAb A formulations at 25 mg/mL and 10 mg/mL in amorphous formulation was in the range of 1 to 3 min. Finally, for amorphous-crystalline formulation, for both mAb A and Pro B at 2.5 and 25 mg/mL protein concentration, the reconstitution time range was 0.5 to 2 min. Increase in reconstitution time with increase in protein concentration from 2.5 to 50 mg/mL is in line with the literature reports.[9] However, the range for reconstitution time was the same for both the control and single-step drying cycle across all 3 protein concentrations (i.e., 10, 25, and 50 mg/mL) in amorphous formulation and in amorphous-crystalline formulation (i.e., at 2.5 and 25 mg/mL protein concentration) suggesting no impact of processing condition on reconstitution time.

Table 2
Aggregation Rates for Lyophilized Drug Product

Protein[a]	Protein Concentration (mg/mL)	Cycle ID[b]	Aggregation Rate (% Aggregates/mo)	
			5°C[c]	40°C[d]
Amorphous-Only Formulation				
mAb A	50	50-A-SS	0.003	0.26
		50-A-C	0.001	0.27
mAb A	25	25-A-SS	0.000	0.08
		25-A-C	0.000	0.15
mAb A	10	10-A-SS	0.000	0.00
		10-A-C	0.000	0.02
Pro B	50	50-B-SS	0.000	0.15
		50-B-C	0.002	0.15
Amorphous-Crystalline Formulation				
mAb A	2.5	2.5-AC-SS	0.00	0.05
		2.5-AC-C	0.00	0.1
mAb A	25	25-AC-SS	0.00	0.73
		25-AC-C	0.00	0.74
Pro B	2.5	2.5-BC-SS	0.00	0.4
		2.5-BC-C	0.00	0.4
Pro B	25	25-BC-SS	0.10	11.0
		25-BC-C	0.10	11.5

[a] mAb A is an IgG1 monoclonal antibody. Pro B is a fusion protein with a molecular weight of ~90 kDa.

[b] Cycle ID key: C, control; L, laboratory scale; P, pilot scale; R, ramp rate; S, single-step drying; A, mAb A; B, Pro B; AC, BC, mAb A and Pro B in amorphous-crystalline formulation, respectively.

[c] Aggregation rate at 5°C was determined based on time points T = 0, 1, 2, 4, 9, 12, and 42 mo for amorphous-only formulations, whereas for amorphous-crystalline formulations, aggregation rate at 5°C was determined based on time points T = 0, 1, 2, 3, 6, 9, 12, and 26 mo.

[d] Lyophilized drug product stored for 1 mo for amorphous-only formulation and stored for 2 mo for amorphous-crystalline formulation. Relatively, higher aggregation rates were observed at 40°C for 25 mg/mL mAb A and Pro B in amorphous-crystalline formulation due to lower lyoprotectant concentration (i.e., 1% [w/v] disaccharide for 25 mg/mL of protein).

Results for Physical and Chemical Stabilities and Potency

Drug product from the single-step drying and control cycles showed no significant difference in the physical stability measured by HPSEC for mAb A and Pro B at different protein concentrations (Table 2). In addition, SVP analysis performed by MFI showed no significant difference in SVP for up to 3.5 and 2 years for amorphous and amorphous-crystalline formulation matrix, respectively, for control and single-step drying samples (Table 3). In addition, bioassay results showed no impact of drying conditions on potency for mAb A and Pro B (Table 4). In addition, chemical stability testing using cIEF for Pro B showed comparable results for single-step drying and control cycles (Table 5).

Effect of Vial Size

Different size of vials has a significant impact on the lyophilization unit operation. Comparison of various vial sizes for the freeze-drying process has been discussed in the literature.[40,41] It was reported that large diameter vials (e.g., 10R, 20R, 30R, and 50R vials) with a constant fill volume resulted in lower product resistance and drying time compared to smaller diameter vials (e.g., 2R) due to fill depth differences.[40] However, the penalty for using larger diameter vials is a decrease in the number of vials a lyophilizer can accommodate compared to smaller diameter vials.[40] In the present study, different vial sizes (3 mL, 10 mL, and 20 mL; cycle IDs: 50-A-SS, 50-B-10, and 50-B-20, respectively) were studied for single-step drying at a 50 mg/mL amorphous-only formulation by keeping the fill depth or product height constant. Smaller diameter vials (3-mL) showed the presence of product shrinkage, whereas larger diameter vials (10-mL and 20-mL) showed cracking for the lyophilized product with ~1 cm product height. Product shrinkage and cracking has been reported for formulations containing disaccharides (e.g., trehalose and sucrose). This shrinkage and cracking was dependent on a number of factors, including the level of unfrozen water (W_g') associated with the disaccharides, the vial type, and the freezing protocol.[39,42-44] Product shrinkage was reported[39] greater for smaller diameter 2R vials compared to larger diameter 10R vials, whereas cracking was higher for larger diameter 10R vials compared to smaller diameter 2R vials, which is consistent with the results of the present study.

Effect of Fill Height

For the single-step drying process, lyophilized product for Pro B at a 50 mg/mL concentration with a 3.3 mL fill volume in a 10-mL vial (fill height ~1.0 cm, cycle ID: 50-B-3.3) showed no product collapse. However, a 7.7 mL fill in a 10-mL vial (fill height of ~2.5 cm, cycle ID: 50-B-7.7) resulted in partial collapse. In addition, as expected, fill height of 2.5 cm resulted in a longer drying time compared to a 1.0 cm fill height (Table 1). Thus, fill height is an important factor impacting not only process efficiency (drying time) but also product quality (product appearance).

Effect of Scale

The single-step drying process (Table 1, cycle ID: 50-B-SS) for Pro B on a pilot-scale lyophilizer resulted in elegant appearance. In addition, single-step drying with a T_s of 40°C showed a significant reduction (~43%) in drying time compared to the control cycle (Table 1). In addition, the single-step drying process for mAb C on laboratory- and pilot-scale lyophilizers resulted in comparable drying times although the batch size and percent load of lyophilizer capacity were significantly different (the % load for laboratory- and pilot-scale lyo runs were 25% and 8%, respectively). The similar drying times for laboratory- and pilot-scale freeze-drying runs indicate a decrease in radiation effects for the single-step drying process, which is a significant advantage, for process scale-up and technology transfer, over the traditional 2-step drying approach. The reduction in the edge vial effect is due to the higher T_s (≥40°C) used for the single-step drying (i.e., relatively less contribution from radiation heat transfer at higher shelf temperature).[38]

Table 3
Subvisible Particle Analysis Using MFI for Lyophilized Drug Product

Protein[a]	Protein Concentration (mg/mL)	Cycle ID[b]	Time Point (y)	Increase in SVP Count (counts/mL) Compared to T0[c]		
				≥2 μm	≥10 μm	≥25 μm
Amorphous-only formulation						
mAb A	50	50-A-SS	3.5	3598	0	0
		50-A-C		72	0	0
mAb A	25	25-A-SS	3.5	727	166	7
		25-A-C		452	144	1
mAb A	10	10-A-SS	3.5	0	76	11
		10-A-C		1822	115`	20
Pro B	50	50-B-SS	3.5	665	23	4
		50-B-C		241	0	8
Amorphous-crystalline formulation						
mAb A	2.5	2.5-AC-SS	2	34	0	4
		2.5-AC-C		0	0	5
mAb A	25	25-AC-SS	2	0	0	0
		25-AC-C		375	98	3
Pro B	2.5	2.5-BC-SS	2	501	38	15
		2.5-BC-C		0	0	0
Pro B	25	25-BC-SS	2	0	0	0
		25-BC-C		0	0	0

[a] mAb A is an IgG1 monoclonal antibody. Pro B is a fusion protein with a molecular weight of ~ 90 kDa.
[b] Cycle ID key: C, control; L, laboratory scale; P, pilot scale; R, ramp rate; S, single-step drying; A, mAb A; B, Pro B; AC, BC, mAb A and Pro B in amorphous-crystalline formulation, respectively.
[c] Increase in SVP count was determined by subtracting T0 SVP count from end of stability samples (i.e., T = 3.5 and 2 y for amorphous and amorphous-crystalline formulations, respectively). SVP count of 0 indicates that there was no increase in SVP count compared to T0.

Table 4
Bioassay (% Relative Potency) Results for Lyophilized Drug Product

Protein[a]	Protein Concentration (mg/mL)	Cycle ID[b]	Time (mo) at 2°C-8°C	Bioassay Results (% Relative Potency) 2°C-8°C
Amorphous-Only Formulation				
mAb A	50	Pre-lyo	0	125
		50-A-SS	12	101
		50-A-C	12	105
mAb A	10	Pre-lyo	0	99
		10-A-SS	12	99
		10-A-C	12	96
Pro B	50	Pre-lyo	0	101
		50-B-SS	12	96
		50-B-C	12	99
Amorphous-Crystalline Formulation				
mAb A	2.5	2.5-AC-SS	0	102
		2.5-AC-SS	6	102
		2.5-AC-C	0	104
		2.5-AC-C	6	106
mAb A	25	25-AC-SS	0	98
		25-AC-SS	6	96
		25-AC-C	0	95
		25-AC-C	6	99
Pro B	2.5	2.5-AC-SS	0	99
		2.5-AC-SS	6	98
		2.5-AC-C	0	95
		2.5-AC-C	6	96
Pro B	25	25-AC-SS	0	94
		25-AC-SS	6	93
		25-AC-C	0	93
		25-AC-C	6	93

[a] mAb A is an IgG1 monoclonal antibody. Pro B is a fusion protein with a molecular weight of ~ 90 kDa.
[b] Cycle ID key: C, control; L, laboratory scale; P, pilot scale; R, ramp rate; S, single-step drying; A, mAb A; AC, mAb A in amorphous-crystalline formulation, respectively.

Effect of Ramp Rate

For mAb A at 50 mg/mL, the single-step drying process with (cycle ID: 50-A-R) a 0.1°C/min drying ramp rate resulted in a reduction of product shrinkage compared to the 0.5°C/min ramp rate (cycle ID: 50-A-SS) single-step drying and control cycles. However, the 0.1°C/min drying ramp rate also resulted in about 4-fold increase in drying time compared to the 0.5°C/min ramp rate (Table 1), thus defeating the purpose of the single-step drying approach. In addition, a slower ramp rate, for single-step drying, may reduce the extent of product shrinkage but does not eliminate it completely.

Why Single-Step Drying Is Feasible? (Correlation of $T_{p,max}$, T_p, and % Water Content)

For single-step drying process, 2 distinct drying phases (primary and secondary) are observed as shown by the dark and faint shaded regions in Figure 3. The shaded region indicates primary drying phase, in which T_p increased with T_s during the drying ramp before reaching a steady state. The steady-state T_p was observed for a very short time for edge and center vial thermocouples. After completion of the T_s ramp to 60°C and a hold of 1 h, the T_p started increasing, which indicates that the primary drying is about to complete. The primary drying phase showed minimal difference

Table 5
Relative % of Acidic, Main, and Basic Species as Determined by cIEF for Pro B

Protein[a]	Protein Concentration (mg/mL)	Cycle ID[b]	Time (mo) at 2°C-8°C	cIEF (% Basic, %Main, %Acidic)
Amorphous-only formulation				
Pro B	50	Pre-lyo	0	0, 84.0, 16.0
		50-B-SS	12	0, 84.8, 15.2
		50-B-C	12	0, 85.2, 14.8
Amorphous-crystalline formulation				
Pro B	2.5	2.5-AC-SS	0	0, 72.6, 27.4
		2.5-AC-SS	6	0, 74.7, 25.3
		2.5-AC-C	0	0, 75.9, 24.1
		2.5-AC-C	6	0, 76.1, 23.9
Pro B	25	25-AC-SS	0	0, 83.9, 16.1
		25-AC-SS	6	0, 82, 18.0
		25-AC-C	0	0, 87.2, 12.8
		25-AC-C	6	0, 84.7, 15.3

[a] mAb A is an IgG1 monoclonal antibody. Pro B is a fusion protein with a molecular weight of ~ 90 kDa.
[b] Cycle ID key: C, control; L, laboratory scale; P, pilot scale; R, ramp rate; S, single-step drying; A, mAb A; AC, mAb A in amorphous-crystalline formulation, respectively.

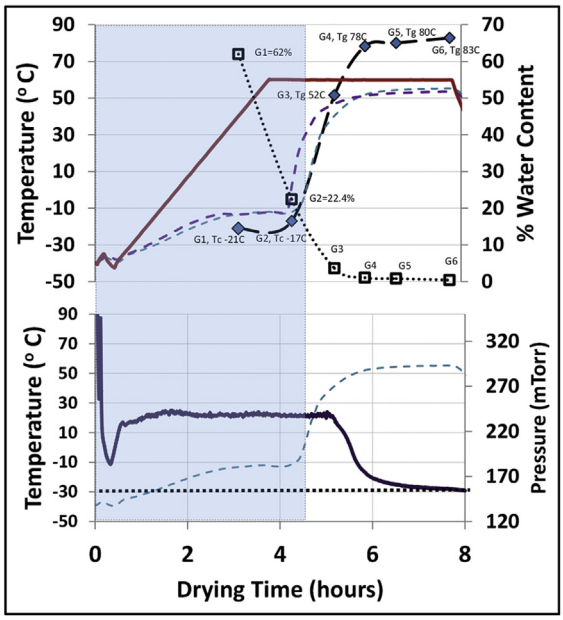

Figure 3. Correlation of $T_{p,max}$ (i.e., T_c for primary drying portion [shaded region] and T_g for secondary drying portion of single-step drying), T_p and % water content using mAb A at 50 mg/mL in a 3 mL vial. Top graph is showing T_p (dashed line) for warmest and coldest representative thermocouple vial, $T_{p,max}$ curve (long dashed line, filled diamonds) and % water content (dotted line, open squares), T_s (solid line) during various time points for single-step drying. Bottom graph is showing CM (dotted line) and the Pirani gauge (solid line) results during drying step and comparison with product temperature (T_p) (dashed line).

(<30 min) to completion between the center (coldest) and edge (warmest) product temperatures. In addition, the Pirani pressure showed a steep drop after completion of drying. The minimal difference in the T_p (center and edge) and the steep Pirani pressure drop indicate homogeneity in the drying rate for the single-step drying process (Fig. 3).

The percent water content was evaluated during the single-step drying process at various time points. In general, ~20% water is present at the end of the primary drying.[34,45] Vials G1 and G2 showed >20% water (62% and 22.4%, respectively) and lack of dried product, which indicates that the primary drying phase of the single-step drying process was not completed yet (Fig. 3). Vials G3, G4, G5, and G6 showed the presence of partially dried product with ≤20% residual water, which confirms the secondary drying phase (product appearance similar to Fig. 2, 50 mg/mL single-step drying cycle). Thus, although from a process standpoint drying is carried out in a single step, there are still 2 distinct phases of drying, wherein ice is first removed by sublimation and then unfrozen water is removed by desorption.

The T_c for G1 vial was similar to the T_c of the prelyo sample G0 ($T_c = -21°C$), which is due to the presence of most of the water (62%) in the vial (Fig. 3). The T_c for the G2 vial was higher ($T_c = -17°C$) compared to G1, which is due to removal of water from the vial as drying progresses (water content for G2 = 22.4%). Removal of water during primary drying does not change T_g' of the solution as the solutes are concentrated in the same proportion.[34,45-47] Determination of T_g' for samples G0, G1, and G2 confirmed no change in T_g' with water removal during drying. In addition, internal data (unpublished) support the trend that the T_g' of the solution remained constant, whereas the T_c increased by about 10°C for increasing the protein concentration from 25 to 85 mg/mL, as long as the ratio of protein to excipient in the formulation was kept constant. The thermal properties T_c and T_g' may have different trends due to differences in physical properties measured. The T_g' measurement using DSC is based on a change in the heat capacity associated with glass transition, whereas the T_c measurement using FDM is based on viscous flow.[34,48]

The T_c, measured by FDM, for G1 and G2 was lower than the T_p, which indicates that drying was performed above the T_c for the primary drying phase of single-step drying and still resulted in an intact dried product. Drying above T_c without collapse may be feasible because the T_c measured by FDM is not representative of the collapse in a vial, and the T_c in a vial may be few degrees higher as discussed earlier.[18-20] Alternatively, the time scale of the experiment (i.e., drying phase [T = 8 h] of single-step drying cycle) may be too short to cause any visible collapse, although microcollapse may be present.[48] In addition, as reported in litereature,[9,12] for amorphous formulations with protein concentration ≥50 mg/mL, there is a significant difference (≥4°C) observed between T_c and T_g'. In authors' opinion, there is no viscous flow for drying above T_c for 50 mg/ml formulation due to high viscosity. Measuring viscosity changes for the frozen system during primary drying phase (i.e., G1 and G2 vials) of single-step drying cycle may provide the definitive answer. However, there are practical limitations for measuring the viscosity of the frozen system due to presence of ice.[49] In addition, as per literature,[48] the collapse temperature increases with the sublimation rate, and single-step drying process is associated with higher sublimation rates, which may also prevent collapse for the lyophilized product.

For the secondary drying phase of single-step drying, the T_g measured for partially dried product from vials G3, G4, G5, and G6 was greater than the corresponding T_p during drying (Fig. 3). As expected, the T_g increased from G3 to G5 as drying progressed due to further removal of residual water. Therefore, the effective $T_{p,max}$ (i.e., the T_c and T_g for primary and secondary drying phases, respectively) increased as drying progressed due to removal of water (Fig. 3), thereby allowing drying at a high T_p ($T_p > T_c$) without product collapse.

Removal of water during primary and secondary drying phases of the single-step drying may also explain the lack of protein denaturation and stability impact observed for performing drying at 60°C. As shown in Figure 3, during the primary drying phase (shaded region), most of the ice is still present, and the sublimation cooling effect keeps the product at a relatively low temperature (<−10°C) even for a shelf temperature of 60°C. At the start of the secondary drying phase (nonshaded region) of single-step drying, partially dried product is formed with <20% water content (i.e., for G3 water content is 3.7%), and protein denaturation is not an issue in such a relatively dry solid state for drying temperatures below 100°C.[10]

Scale-Up Considerations

Performing single-step drying is feasible on laboratory- and pilot-scale lyophilizers (Table 1, cycle IDs: 50-MC-L, 50-MC-P). However, there are several challenges for scaling-up and transferring the single-step freeze-drying process from laboratory to production scale. For the single-step drying process, most of the drying is completed during the ramp phase (i.e., nonsteady state process), and hence, modeling the process could be a significant challenge. In addition, the production freeze dryers may have following limitations:

(1) Unable to achieve and maintain a high shelf temperature (T_s ≥ 40°C) throughout the drying step.
(2) Limited condenser capacity[50,51]: Unable to support the high sublimation rate associated with single-step drying and resulting in an out-of-control process. In this case, condenser temperature may increase significantly during single-step drying.
(3) Choked flow: Depending on the geometry and design of the freeze dryer, the process can get out of control due to choked

flow.[36,52,53] In this case, condenser temperature does not change much, but condenser pressure drops significantly.[36,52,53]

Therefore, before implementation of single-step drying at production scale, it is critical to understand the limitations and capabilities of the freeze dryer.[37,51,54]

Case Study Illustrating Scale-Up Considerations for Single-Step Drying Process

For a hypothetical example using model protein Pro B, single-step drying process with a sublimation rate of ~3 kg/h would result in $P_{c,min}$ (based on choked flow limitation) of ~80m Torr on Dryer-A (Fig. 4). Clearly, chamber pressure set point of 80 mTorr would result in out-of-control process. In this case, how to rationally select chamber pressure set point? Given that each freeze dryer has certain control capabilities in terms of temperature and pressure control, and the fact that temperature and pressure excursion could likely occur on production dryer, enough safety margin needs to be built-in when selecting chamber pressure set point. Considering a worst-case pressure control range of ±30 mTorr for dryer A, a chamber pressure set point of ≥120 mTorr would enable to perform single-step drying without out-of-control process.

Summary

A significant reduction (at least 40%) in lyophilization process time was achieved with laboratory- and pilot-scale freeze dryers using a single-step drying approach compared to the 2-step drying process with aggressive drying conditions (primary drying above T_g'[8,9]). Single-step drying for an amorphous-only formulation showed product shrinkage and partial collapse for low protein concentration formulations (≤25 mg/mL), whereas a high protein concentration formulation (≥50 mg/mL) showed minor product shrinkage. For low protein concentration formulations (≤25 mg/mL), the addition of a crystallizing excipient improved product appearance. With the single-step drying process, there was no impact on product quality for different model proteins at various protein concentrations in amorphous-only and amorphous-crystalline formulations. Although single-step drying showed no product quality impact for the model proteins evaluated in these case studies, still individual protein and formulation considerations such as protein concentration, excipients, and formulation matrix need to be evaluated for impact of single-step drying process. In addition, fill height and vial type had significant impact on product appearance for the single-step drying process. An increase in fill height resulted in product shrinkage and partial collapse. A lower diameter vial (3 mL) showed product shrinkage, whereas larger diameter vials (10 and 20 mL) showed cracking. Comparison of maximum allowable product temperature ($T_{p,max}$), product temperature (T_p), and percent water content showed an increase in the $T_{p,max}$ as water was removed during the drying step. An increase in $T_{p,max}$ during drying allows single-step drying to be performed at higher T_s and hence higher T_p. A significant benefit of single-step drying was homogeneous drying due to decreased radiation effect. Laboratory- and pilot-scale single-step drying runs with different lot sizes showed comparable drying times indicating a lower radiation effect. However, for the single-step drying process, most of the drying was completed during the ramp phase (i.e., during a nonsteady state heat and mass transfer). Therefore, scale-up and transfer of the single-step drying process from laboratory- to pilot-scale to commercial scale needs to be carefully evaluated. In addition, the single-step drying process may have scale-up challenges such as choked flow and condenser overload. For successful implementation of single-step drying at clinical and commercial scales, production lyophilizer specifications and process characterization information are critical and should be evaluated for the single-step drying process.

If short freeze-drying times (≤2 days) are achieved without adversely affecting product quality, then significant reduction in lyophilization process cost can be achieved. Potentially, single-step drying can reduce the gap in the overall production cost and time for the manufacturing of lyophilized products compared to liquid products and alternate technologies (e.g., spray-drying and microwave drying). In addition, short lyophilization times using a single-step drying approach may give scheduling flexibility for drug product manufacturing, low probability of equipment failure, and increased throughput. However, the major limitation for using the lyophilization process is the lot size. Lyophilized drug product manufacturing is constrained by the shelf surface area and capacity of the production lyophilizer due to the batch mode of the freeze-drying unit operation. Recent advances in continuous freeze-drying have the potential to remove the batch size limitation associated with the lyophilization process.[55-57] Continuous freeze-drying may become a reality for drug product manufacturing in the future. However, significant work is still required before continuous freeze-drying can be implemented for clinical and commercial manufacturing of biopharmaceuticals. Until then, single-step drying may be a cost-effective and high-throughput approach for the manufacturing of biologics. As the single-step drying approach with a 1-day cycle time is becoming a reality, the lyophilizer and not the formulation is now becoming the limiting factor for the lyophilization process design space. Therefore, manufacturers of clinical- and commercial-scale lyophilizer need to consider and implement the instrument design changes that may be required to support a single-step freeze-drying process.

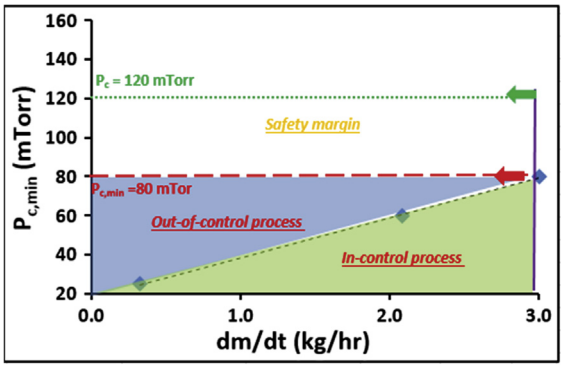

Figure 4. Case study results for comparison of $P_{c,min}$ and sublimation rate (dm/dt) using Pro B as a model protein at 50 mg/mL.

Acknowledgments

The authors thank Chirag Mevawala for the laboratory support and Nancy Craighead for the editorial support of the article.

References

1. Pikal M. Freeze drying. In: Swarbrick J, ed. *Encyclopedia of Pharmaceutical Technology, ENCL 100001712*. New York: Marcel Dekker Inc; 2001:1299.
2. Patel SM, Nail SL, Pikal MJ, et al. Lyophilized drug product cake appearance: what is acceptable? *J Pharm Sci*. 2017;106(7):1706-1721.
3. Walters RH, Bhatnagar B, Tchessalov S, Izutsu K, Tsumoto K, Ohtake S. Next generation drying technologies for pharmaceutical applications. *J Pharm Sci*. 2014;103(9):2673-2695.
4. Aniket, Gaul DA, Rickard DL, Needham D. Microglassification: a novel technique for protein dehydration. *J Pharm Sci*. 2014;103(3):810-820.

5. Abdul-Fattah AM, Kalonia DS, Pikal MJ. The challenge of drying method selection for protein pharmaceuticals: product quality implications. *J Pharm Sci*. 2007;96(8):1886-1916.
6. Maltesen MJ, van de Weert M. Drying methods for protein pharmaceuticals. *Drug Discov Today Technol*. 2008;5(2-3):e81-e88.
7. Jangle RD, Pisal SS. Vacuum foam drying: an alternative to lyophilization for biomolecule preservation. *Indian J Pharm Sci*. 2012;74(2):91-100.
8. Pansare S, DePaz R, Patel S. *SMi's Pharmaceutical Lyophilization & Freeze Drying Conference*. Poster presentation; 2015.
9. Depaz RA, Pansare S, Patel SM. Freeze-drying above the glass transition temperature in amorphous protein formulations while maintaining product quality and improving process efficiency. *J Pharm Sci*. 2016;105(1):40-49.
10. Tang X, Pikal MJ. Design of freeze-drying processes for pharmaceuticals: practical advice. *Pharm Res*. 2004;21(2):191-200.
11. Patel SM, Doen T, Pikal MJ. Determination of end point of primary drying in freeze-drying process control. *AAPS PharmSciTech*. 2010;11(1):73-84.
12. Colandene JD, Maldonado LM, Creagh AT, Vrettos JS, Goad KG, Spitznagel TM. Lyophilization cycle development for a high-concentration monoclonal antibody formulation lacking a crystalline bulking agent. *J Pharm Sci*. 2007;96(6):1598-1608.
13. Bellows RJ, King CJ. Freeze-drying of aqueous solutions: maximum allowable operating temperature. *Cryobiology*. 1972;9(6):559-561.
14. Passot S, Fonseca F, Barbouche N, et al. Effect of product temperature during primary drying on the long-term stability of lyophilized proteins. *Pharm Dev Technol*. 2007;12(6):543-553.
15. Schersch K, Betz O, Garidel P, Muehlau S, Bassarab S, Winter G. Systematic investigation of the effect of lyophilizate collapse on pharmaceutically relevant proteins I: stability after freeze-drying. *J Pharm Sci*. 2010;99(5):2256-2278.
16. Schersch K, Betz O, Garidel P, Muehlau S, Bassarab S, Winter G. Systematic investigation of the effect of lyophilizate collapse on pharmaceutically relevant proteins III: collapse during storage at elevated temperatures. *Eur J Pharm Biopharm*. 2013;85(2):240-252.
17. Schersch K, Betz O, Garidel P, Muehlau S, Bassarab S, Winter G. Systematic investigation of the effect of lyophilizate collapse on pharmaceutically relevant proteins, part 2: stability during storage at elevated temperatures. *J Pharm Sci*. 2012;101(7):2288-2306.
18. Greco K, Mujat M, Galbally-Kinney KL, et al. Accurate prediction of collapse temperature using optical coherence tomography-based freeze-drying microscopy. *J Pharm Sci*. 2013;102(6):1773-1785.
19. Mujat M, Greco K, Galbally-Kinney KL, et al. Optical coherence tomography-based freeze-drying microscopy. *Biomed Opt Express*. 2012;3(1):55-63.
20. Korang-Yeboah M, Srinivasan C, Siddiqui A, Awotwe-Otoo D, Cruz CN, Muhammad A. Application of optical coherence tomography freeze-drying microscopy for designing lyophilization process and its impact on process efficiency and product quality. *AAPS PharmSciTech*. 2018;19:448-459.
21. Kramer T, Kremer DM, Pikal MJ, Petre WJ, Shalaev EY, Gatlin LA. A procedure to optimize scale-up for the primary drying phase of lyophilization. *J Pharm Sci*. 2009;98(1):307-318.
22. Koganti VR, Shalaev EY, Berry MR, et al. Investigation of design space for freeze-drying: use of modeling for primary drying segment of a freeze-drying cycle. *AAPS PharmSciTech*. 2011;12(3):854-861.
23. Chen X, Sadineni V, Maity M, Quan Y, Enterline M, Mantri RV. Finite element method (FEM) modeling of freeze-drying: monitoring pharmaceutical product robustness during lyophilization. *AAPS PharmSciTech*. 2015;16(6):1317-1326.
24. Giordano A, Barresi AA, Fissore D. On the use of mathematical models to build the design space for the primary drying phase of a pharmaceutical lyophilization process. *J Pharm Sci*. 2011;100(1):311-324.
25. Bjelošević M, Seljak KB, Trstenjak U, Logar M, Brus B, Ahlin Grabnar P. Aggressive conditions during primary drying as a contemporary approach to optimise freeze-drying cycles of biopharmaceuticals. *Eur J Pharm Sci*. 2018;122:292-302.
26. Lewis LM, Johnson RE, Oldroyd ME, et al. Characterizing the freeze-drying behavior of model protein formulations. *AAPS PharmSciTech*. 2010;11(4):1580-1590.
27. Tang XC, Nail SL, Pikal MJ. Freeze-drying process design by manometric temperature measurement: design of a smart freeze-dryer. *Pharm Res*. 2005;22(4):685-700.
28. Horn J, Schanda J, Friess W. Impact of fast and conservative freeze-drying on product quality of protein-mannitol-sucrose-glycerol lyophilizates. *Eur J Pharm Biopharm*. 2018;127:342-354.
29. Chang BS, Fischer NL. Development of an efficient single-step freeze-drying cycle for protein formulations. *Pharm Res*. 1995;12(6):831-837.
30. Carpenter JF, Chang BS, Garzon-Rodriguez W, Randolph TW. Rational design of stable lyophilized protein formulations: theory and practice. *Pharm Biotechnol*. 2002;13:109-133.
31. Chatterjee K, Shalaev EY, Suryanarayanan R. Partially crystalline systems in lyophilization: II. Withstanding collapse at high primary drying temperatures and impact on protein activity recovery. *J Pharm Sci*. 2005;94(4):809-820.
32. Stärtzel P, Gieseler H, Gieseler M, et al. Mannitol/l-Arginine-Based formulation systems for freeze drying of protein pharmaceuticals: effect of the l-arginine counter ion and formulation composition on the formulation properties and the physical state of mannitol. *J Pharm Sci*. 2016;105(10):3123-3135.
33. Pansare S, Patel S, Lobo B, Shah A. *2013 Colorado Protein Stability Conference*. Poster presentation; 2013.
34. Pansare SK, Patel SM. Practical considerations for determination of glass transition temperature of a maximally freeze concentrated solution. *AAPS PharmSciTech*. 2016;17(4):805-819.
35. Esfandiary R, Gattu SK, Stewart JM, Patel SM. Effect of freezing on lyophilization process performance and drug product cake appearance. *J Pharm Sci*. 2016;105(4):1427-1433.
36. Patel SM, Chaudhuri S, Pikal MJ. Choked flow and importance of mach I in freeze-drying process design. *Chem Eng Sci*. 2010;65(21):5716-5727.
37. Ganguly A, Alexeenko AA, Schultz SG, Kim SG. Freeze-drying simulation framework coupling product attributes and equipment capability: toward accelerating process by equipment modifications. *Eur J Pharm Biopharm*. 2013;85(2):223-235.
38. Rambhatla S, Pikal MJ. Heat and mass transfer scale-up issues during freeze-drying, I: atypical radiation and the edge vial effect. *AAPS PharmSciTech*. 2003;4(2):E14.
39. Ullrich S, Seyferth S, Lee G. Measurement of shrinkage and cracking in lyophilized amorphous cakes. Part I: final-product assessment. *J Pharm Sci*. 2015;104(1):155-164.
40. Liu J, Viverette T, Virgin M, Anderson M, Paresh D. A study of the impact of freezing on the lyophilization of a concentrated formulation with a high fill depth. *Pharm Dev Technol*. 2005;10(2):261-272.
41. Pikal MJ, Roy ML, Shah S. Mass and heat transfer in vial freeze-drying of pharmaceuticals: role of the vial. *J Pharm Sci*. 1984;73(9):1224-1237.
42. Ullrich S, Seyferth S, Lee G. Measurement of shrinkage and cracking in lyophilized amorphous cakes, part 3: hydrophobic vials and the question of adhesion. *J Pharm Sci*. 2015;104(6):2040-2046.
43. Rambhatla S, Obert JP, Luthra S, Bhugra C, Pikal MJ. Cake shrinkage during freeze drying: a combined experimental and theoretical study. *Pharm Dev Technol*. 2005;10(1):33-40.
44. Ullrich S, Seyferth S, Lee G. Measurement of shrinkage and cracking in lyophilized amorphous cakes. Part IV: effects of freezing protocol. *Int J Pharm*. 2015;495(1):52-57.
45. Liu J. Physical characterization of pharmaceutical formulations in frozen and freeze-dried solid states: techniques and applications in freeze-drying development. *Pharm Dev Technol*. 2006;11(1):3-28.
46. Fox TG, Loshaek S. Influence of molecular weight and degree of crosslinking on the specific volume and glass temperature of polymers. *J Polym Sci*. 1955;15(80):371-390.
47. Fox T, Flory P. Second-order transition temperatures and related properties of polystyrene. I. Influence of molecular weight. *J Appl Phys*. 1950;21(6):581.
48. Pikal MJ, Shah S. The collapse temperature in freeze-drying - dependence on measurement methodology and rate of water removal from the glassy phase. *Int J Pharm*. 1990;62(2-3):165-186.
49. Gu JH, Beekman A, Wu T, et al. Beyond glass transitions: studying the highly viscous and elastic behavior of frozen protein formulations using low temperature rheology and its potential implications on protein stability. *Pharm Res*. 2013;30(2):387-401.
50. Searles J. Optimizing the throughput of freeze-dryers within a constrained design space. In: *Freeze-Drying/Lyophilization of Pharmaceutical and Biological Products*. 3rd ed. Boca Raton, FL: CRC Press; 2010:425.
51. Sane SU, Hsu CC. Considerations for successful lyophilization process scale-up, technology transfer, and routine production. In: *Formulation and Process Development Strategies for Manufacturing Biopharmaceuticals*. Hoboken, NJ: John Wiley & Sons Inc; 2010:797.
52. Patel SM, Pikal MJ. Lyophilization process design space. *J Pharm Sci*. 2013;102(11):3883-3887.
53. Patel SM, Lobo B, Shah A. Practical considerations for freeze-drying process design, development and scale-up. *Am Pharm Rev*. 2013;16(6).
54. Rasetto V, Marchisio DL, Fissore D, Barresi AA. On the use of a dual-scale model to improve understanding of a pharmaceutical freeze-drying process. *J Pharm Sci*. 2010;99(10):4337-4350.
55. De Meyer L, Van Bockstal PJ, Corver J, Vervaet C, Remon JP, De Beer T. Evaluation of spin freezing versus conventional freezing as part of a continuous pharmaceutical freeze-drying concept for unit doses. *Int J Pharm*. 2015;496(1):75-85.
56. Van Bockstal PJ, Mortier ST, De Meyer L, et al. Mechanistic modelling of infrared mediated energy transfer during the primary drying step of a continuous freeze-drying process. *Eur J Pharm Biopharm*. 2017;114:11-21.
57. Van Bockstal PJ, De Meyer L, Corver J, Vervaet C, De Beer T. Noncontact infrared-mediated heat transfer during continuous freeze-drying of unit doses. *J Pharm Sci*. 2017;106(1):71-82.